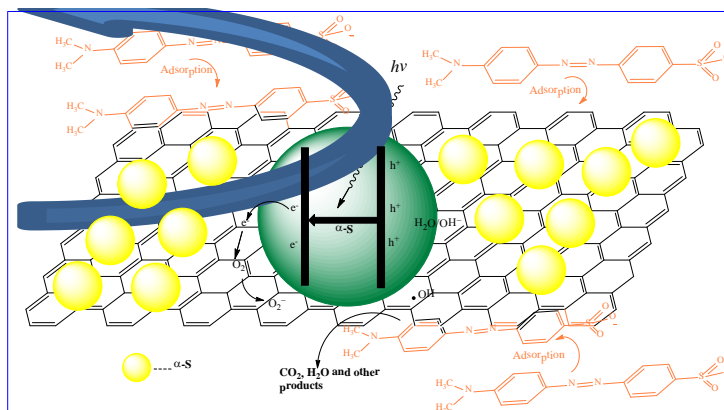**Synthesis of A Sulfur-Graphene Composite as An Enhanced Metal-free Photocatalyst**

Wen-chao Peng and Xiao-yan Li[*]

Environmental Engineering Research Centre, Department of Civil Engineering, The University of Hong Kong, Pokfulam, Hong Kong

[*]Corresponding author. Tel: (852)28592659, Fax: (852)25595337. E-mail: xlia@hkucc.hku.hk

A novel metal-free photocatalyst, sulfur/graphene (S/GR) composite, was synthesized using a facial, one-pot hydrothermal method. The composite showed good activity for the photocatalytic degradation of methyl orange under both UV and solar light.

Research Article

Synthesis of A Sulfur-Graphene Composite as An Enhanced Metal-free Photocatalyst

Wen-chao Peng, and Xiao-yan Li (✉)

Environmental Engineering Research Centre, Department of Civil Engineering, The University of Hong Kong, Pokfulam, Hong Kong

ABSTRACT

A novel metal-free photocatalyst, sulfur/graphene (S/GR) composite, was synthesized using a facial one-pot, two-step hydrothermal method with thiosulfate and graphene oxide (GO) as precursors. A green reductant – l-ascorbic acid was used to transform GO to GR under a mild condition. The photocatalyst powders were characterized by the fourier transform infrared spectroscopy, X-ray diffraction, transmission electron microscopy, scanning electron microscopy, and energy dispersive spectroscopy. Experimental tests were conducted on the photocatalytic decomposition of methyl orange (MO) by the different catalysts. Compared to pure α-S, the as-prepared S/GR composite showed much enhanced photocatalytic activity for the degradation of MO under both UV and solar light The GR addition also greatly increased the hydrophilicity and adsorption capacity of the catalyst material. The results indicate that the incorporation of GR with α-S results in a synergistic effect on the S-based photocatalysts for more effective environmental applications.

KEYWORDS

Metal-free catalyst, α-Sulfur, Graphene, Photocatalysis, Methyl orange, Organic degradation

1. Introduction

The photocatalysis field has been dominated by metal-based materials owing largely to band-gap limitations. A number of metal oxides, metal sulfates, and salts are known to have good photoactivities under UV or visible light [1]. To develop more effective and environmentally friendly photocatalysts, efforts have been made in recent years to apply non-metal materials in the synthesis of new photocatalysts. Silica QDs, red phosphorus, α-sulfur (α-S), and a polymer g-C$_3$N$_4$ are reported to be active for organic photocatalysis or water splitting reactions [2-5]. Among these new metal-free catalysts, α-S shows a great potential owing to its simple facial preparation, good photo-sensitivity with a narrow band-gap (2.79 eV), and high stability [4]. However, in view of its poor hydrophilicity and low reactivity, improvement is

_____

Address correspondence to Xiao-yan Li, xlia@hkucc.hku.hk

still needed for α-S to greatly increase its functionality and efficiency in photocatalytic application [4].

Graphene (GR), a versatile carbon material with a single layer and sp^2-hybridized carbon lattice, possesses excellent electrical, thermal, and mechanical properties [6]. GR has been increasingly used as a support for metals or metal oxides in the fabrication of new catalysts with much enhanced activity [7]. GR is also a new star material in the photocatalysis field, which can serve as an excellent charge carrier at room temperature (200 000 cm^{2}V^{-1}s^{-1}) [8]. Thus, by incorporating GR to form electron-conducting surfaces and channels, the photocatalytic activity of the composite materials can be greatly increased, mainly owing to the effective suppression of the recombination of photo-generated electron–hole pairs [8,9]. Significant improvement has been reported for metal oxides, metal sulfates, and non-metal g-C$_3$N$_4$ by using GR as a synergistic catalyst material [8,10,11]. However, there has been no report on the modification of α-S with GR for making new photocatalysts. In this study, we integrated a small percentage ($\leq$3%) of GR into α-S to fabricate a new metal-free photocatalyst. With the synergistic function of GR, the catalytic activity of α-S was greatly enhanced for the photocatalytic degradation of methyl orange (MO) under both UV and simulated solar (SS) light. Moreover, compared with α-S, the S/GR composite is more modifiable because of its better hydrophilicity and new functional groups, thus other novel photocatalysts can be prepared from the S/GR composite.

2. Materials and Methods

2.1 Preparation of graphite oxide

Hummer's method was used to synthesize graphite oxide from graphite powder [12]. Briefly, graphite (2 g) was mixed with NaNO$_3$ (1 g) in 50 mL concentrated H$_2$SO$_4$ (98%) at 0°C, and KMnO$_4$ (6 g) was then added gently into the system. After being kept at 0°C for 2 h, the mixture was stirred at room temperature for 30 min. Deionized (DI) water (100 mL) was slowly added into the system, while the temperature was kept at 95-98°C for 3 h. The mixture was further treated with 5% H$_2$O$_2$ (50 mL) for 1 h. Finally, graphite oxide formed in the suspension was filtered and washed with DI water, which was then dried at 60°C for 2 d.

2.2 Synthesis of sulfur-graphene (S/GR) composites

Graphite oxide was first exfoliated into graphene oxide (GO) by sonication in DI water [13]. Typically, 24.8 g (0.1 mol) Na$_2$S$_2$O$_3$·5H$_2$O was charged into 100 mL of GO solution at a predetermined concentration (e.g. 0.8 mg/mL for S/GR-1%). The mixture was sonicated for 30 min followed by stirring for 30 min to form a homogenous solution. The solution pH was then adjusted and kept at ~2.0 by adding H$_2$SO$_4$ (30%) every 30 min for 2 h to precipitate sulfur on the surface of the GO. Subsequently, 1.0 g L-ascorbic acid (AA) was added to reduce the GO to graphene (GR). After adjusting the pH to ~9.5 with NaOH (5 wt%), the solution was heated to 85°C for 4 h. After cooling to room temperature, the S/GR composite formed in the solution was washed with DI water and then dried in vacuum at 85°C in an oven. Around 0.5 mg of GR can be generated from 1 mg of GO after the AA reduction. Pure sulfur crystals were synthesized following the same procedure as described above for the S/GR composites, except for the addition of GO into the Na$_2$S$_2$O$_3$ solution and the subsequent reduction process.

2.3 Photocatalytic degradation of methyl orange (MO)

Photodecomposition of methyl orange (MO) was performed in a photo-reactor. For a typical test,

50 mg of photocatalyst was first dispersed in 50 mL of water in a quartz photo-tube by sonication, followed by the addition of MO to an initial concentration of 20 mg/L. Before exposure to light, the suspension was stirred in the dark to allow adsorption of MO by the catalyst powders. According to the color measurement by a UV-vis spectrophotometer (Perkin, Lamda 25), the MO adsorption by the catalysts achieved equilibrium within 30 min. For photocatalysis of MO in an XPA photo-reactor (Xujiang Electromechanical Plant, Nanjing, China), the light source was either a 300 W high pressure mercury lamp for UV light or a 500 W xenon lamp for the simulated solar (SS) light. During the photocatalytic process, 4 mL of the solution was sampled from each photo-tube at regular intervals to monitor the MO concentration change. The sample was withdrawn through a syringe filter (0.2 μm) and the absorbance (ABS) of the filtrate was measured at 463 nm by the UV-visible spectrophotometer as an indication of the MO concentration in the solution.

2.4 Material characterization

The X-ray diffraction (XRD) patterns of the photocatalyst materials were analyzed for their crystal forms by a Bruker D8 Advance X-ray powder diffractometer. The morphology of the catalysts was examined by scanning electron microscopy (SEM) (Hitachi S-4800 FEG SEM, Tokyo, Japan) and transmission electron microscopy (TEM) (Philips Tecnai G220 S-TWIN, Amsterdam, the Netherlands). Fourier transform infrared spectroscopy (FT-IR) (Perkin Elmer, FT-IR Spectrophoeometer Spectrum One B) was used for characterization of the functional groups of different catalysts.

3. Results and Discussion

3.1 Characterization of the photocatalysts

The α-S/GR composites were prepared following a facial one-pot, two-step hydrothermal method. Typically, the graphene oxide (GO) and sodium thiosulfate at a predetermined ratio were dissolved in DI water with sonication to form a homogenous solution [14]. The solution pH was adjusted to ~2, resulting in an S precipitate that deposited on the surface of the GO to form S/GO. Then, l-ascorbic acid (AA) was added to reduce the S/GO to S/GR at 85 °C. AA was selected here for its suitable reducibility and non-toxicity [15].

FT-IR was used to analyze the change in functional groups during the synthesis process (Figure 1a). Pure GR was obtained by the reduction of GO with AA under the same conditions but without the presence of sodium thiosulfate. Abundant oxygen-containing groups can be identified from the FT-IR spectrum of GO, e.g. 1630 cm^{-1} for COO, 1392 cm^{-1} for O-H, and 1085 cm^{-1} for C-O groups, which provide active sites for sulfur precipitation. As shown by the spectrum of GR, almost all of the functional groups were removed by AA reduction in the absence of thiosulfate, indicating the effectiveness of AA for the reduction of GO to GR. With the addition of thiosulfate during the synthesis process, a few new functional groups were produced on the resulting S/GR composite, which appeared to be stable even after the AA reduction. C=S stretching (1220 cm^{-1}) and C–S stretching (1098 cm^{-1}) can be found in the spectrum of S/GR, indicating that S particles are chemically bonded to the GR sheets [14]. These chemical bonds are important to the stability of the S/GR composite.
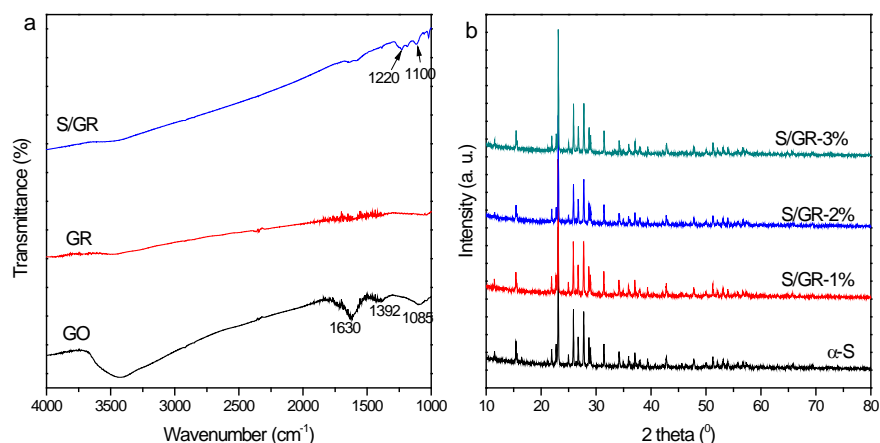
Figure 1 (a) FT-IR profiles of GO, GR, and S/GR composite; (b) XRD patterns of pure α-S and S/GR powders.

XRD analysis was also conducted to determine the crystal form of sulfur (Figure 1b). Typical reflections of α-octa-sulfur (S8, JCPDS#08-0247) were clearly observed for the pure S particles [4,14]. The crystal form of α-S was not affected by the incorporation of GR at different percentages, thus ensuring the photocatalytic activity of α-S in the S/GR composites. No characteristic GR diffraction peaks could be clearly identified from the XRD pattern of S/GR, which might be due to the low amount (≤3 wt%) of GR added and its low diffraction intensity [16].

Figure 2 shows the morphologies of the α-S and S/GR composites at different magnifications. The pure S crystals generally appear to be solid spheres with a diameter as large as 2-3 μm, probably formed by the agglomeration of primary S particles. The addition of GO was shown to decrease the size of S particles. It is apparent that the presence of abundant oxygen-containing groups on the GO surface increased the number of active sites for S precipitation. After the reduction with AA, GO was reduced to GR, and smaller S particles (~1 μm) were found to attach firmly on the GR surface (Figure 2b-c). While the SEM image of S/GR shows only the morphologies of S particles (Figure 2b), both S and GR can be observed from the TEM image (Figure 2c). Despite the small percentage of GR, free GR can still be found at the edge of the S-based composite. Figure 2d at a higher magnification shows the TEM image of free GR at the edge of the composite, in which the typical morphology of chemically reduced GR with obvious wrinkles can be found. The elemental composition of the S/GR composite was further confirmed by the EDS and elemental analyses. Figure 3 presents the elemental mapping results for S and C in the S/GR composite in a selected region (Figure 3a). The yellow dots in Figure 3b indicate sulfur, while the white dots in Figure 3c are carbon. The elemental mapping results confirm that GR was uniformly dispersed over the S/GR composite.
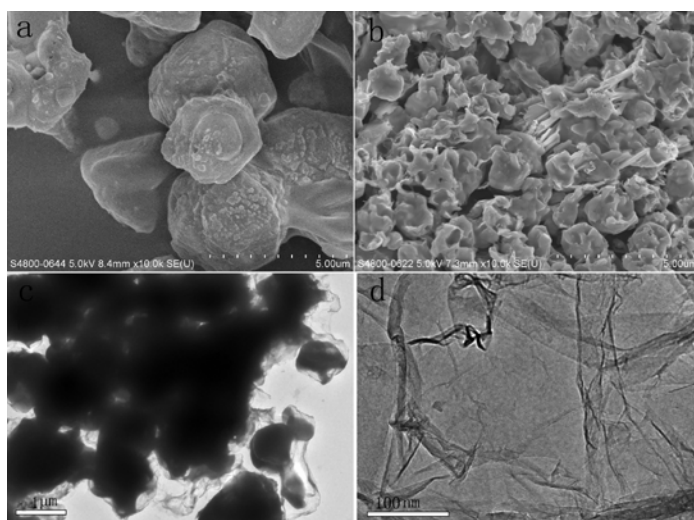
Figure 2 (a) SEM image of pure -S particles, (b) SEM image of the S/GR composite, (c) TEM image of S/GR, and (d) TEM image of GR at the edge of S/GR composite.

Pure α-S has poor hydrophilicity and a low adsorption capacity, which is partially responsible for its low photoactivity in the aqueous phase [4]. The incorporation of GR can greatly improve the hydrophilicity of α-S. Figure 4 displays the dispersion of S/GR composites in water in comparison to α-S particles. While the pure α-S would only stay on top of the water, the S/GR powders could be readily dispersed in water, with sonication of 15 min or so. This increase in hydrophilicity can greatly improve the functionality of the S/GR composites in photocatalysis applications.
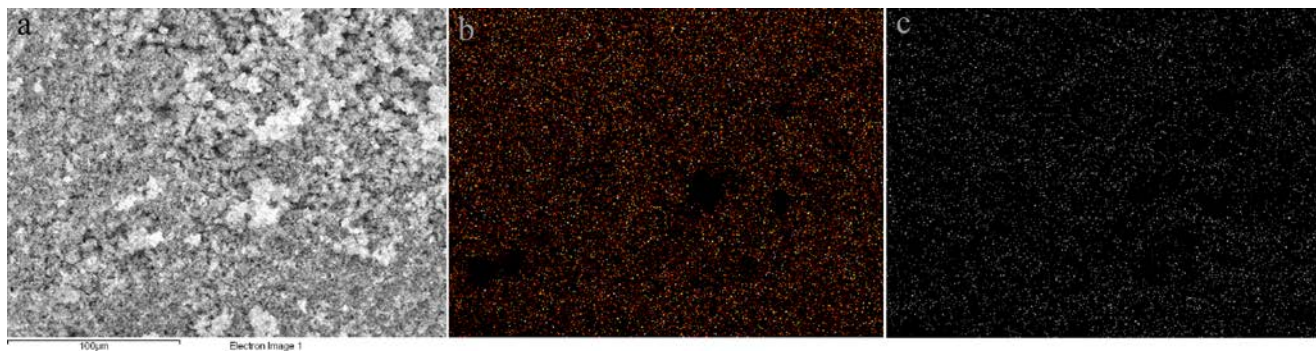

Figure 3 Elemental analysis and N_2-adsorption results for the S/GR-3% composite: (a) SEM image of the mapping area, (b) sulfur Kα mapping, and (c) carbon Kα mapping.
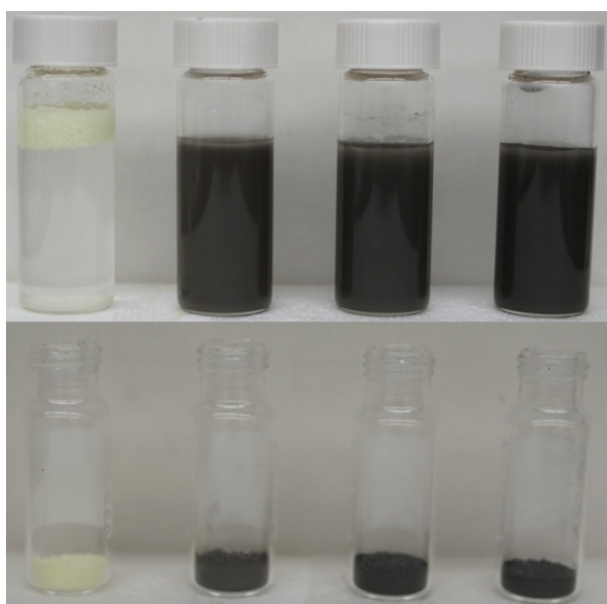
Figure 4 The catalyst powders and suspensions: bottom photo (from left to right) - dry powders of α-S, S/GR-1%, S/GR-2%, and S/GR-3%; top photo - the suspensions of the catalysts in water after sonication

The photocatalytic activities of different catalysts were tested for the degradation of methyl orange (MO), one of the important classes of commercial dyes. MO has often been used as a model dye to test photoredox reactions for decoloring due to the short life of its excited-state and high stability under visible and near UV light [17]. The catalysts with a dosing density of 1 mg/mL were first dispersed in water by sonication, and MO was then added at an initial concentration of 20 mg/L in the photo-tubes. Before exposure to light, the suspensions were stirred in the dark for 30 min to allow MO adsorption by the catalysts. Based on the color comparison in Figure 5, the adsorption capability of the catalysts clearly increased with the addition of GR to the composites. This should be due to the chemical adsorption capacity brought about by the GR and the hydrophilic surface of the catalyst powders after the modification.
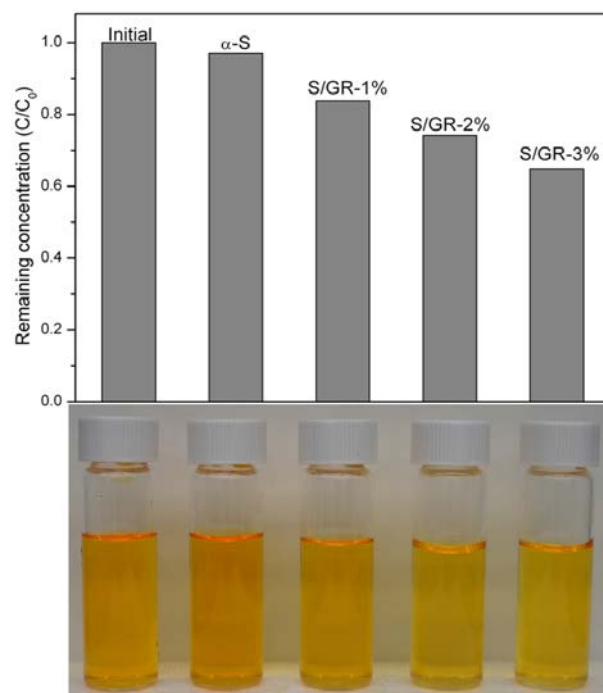
Figure 5 Change of the MO concentration after adsorption by different catalyst materials: top chart - the resulting MO reduction in the solutions; the bottom photo - the appearance of the MO solutions after 30-min adsorption in the dark.

The reductions in MO during the degradation experiments with different photocatalysts are presented in Figure 6, in which C_0 corresponds to the absorbance (ABS) at 463 nm of MO at its original concentration (20 mg/L) and C corresponds to the ABS of MO after a specified test period. The results show that the addition of a small amount of GR can greatly enhance the photocatalytic activity of α-S under both UV and solar radiations. After 3 hr, the S/GR-3% composite in the solution reduced the MO by around 83% and 50% under the UV and SS light, respectively. In contrast, pure α-S reduced the MO by only 14% and 6% under the same test conditions. For decoloring of MO by photocatalysis during the light illumination period, the half-time ($T_{1/2}$) can be determined from the MO reduction curves. Under the UV light, the $T_{1/2}$ of MO for α-S was 883 min, while the $T_{1/2}$ for S/GR-3% was only 122 min. Similarly, the $T_{1/2}$ decreased from 3100 min for α-S to 436 min for S/GR-3% under the SS light.
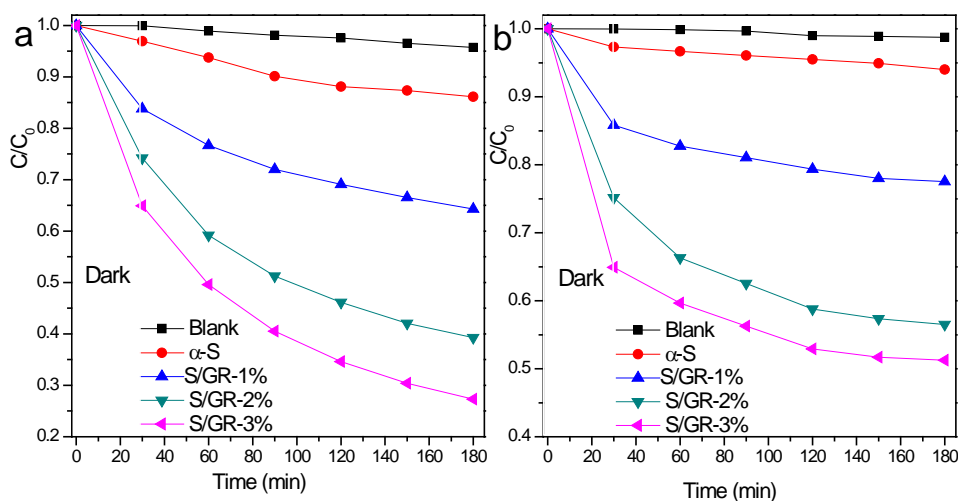
Figure 6 Degradation of methyl orange in the solutions under (a) UV light and (b) simulated solar light by α-S and S/GR composites.
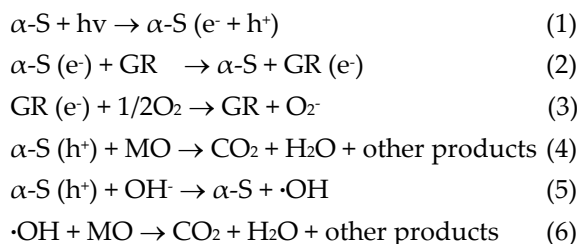
The role of GR in the photocatalytic MO degradation by the α-S/GR composite is illustrated in Figure 7. MO molecules can be readily adsorbed by the aromatic regions of graphene via conjugation, which is beneficial to the subsequent MO degradation [18]. Under UV or SS light, irradiation of photosensitive α-S results in electron excitation and electron–hole pairs. The graphene sheets act as an electron collector to transfer photo-generated electrons from α-S to electron acceptors, e.g. dissolved oxygen, in the aqueous phase to facilitate the electron–hole separation. The holes can directly oxidize MO molecules adsorbed on the catalyst surface. Moreover, the holes may react with water (or hydroxyl) to form hydroxyl free radicals (·OH), which are a strong oxidant for MO decomposition [4]. The degradation of MO would lead to decoloration of the solution and produce CO_2, H_2O, and intermediate products such as phenolic compounds and carboxylic acids. The major reaction steps in the photocatalytic process can be described by the following equations (1–6) [9,19].
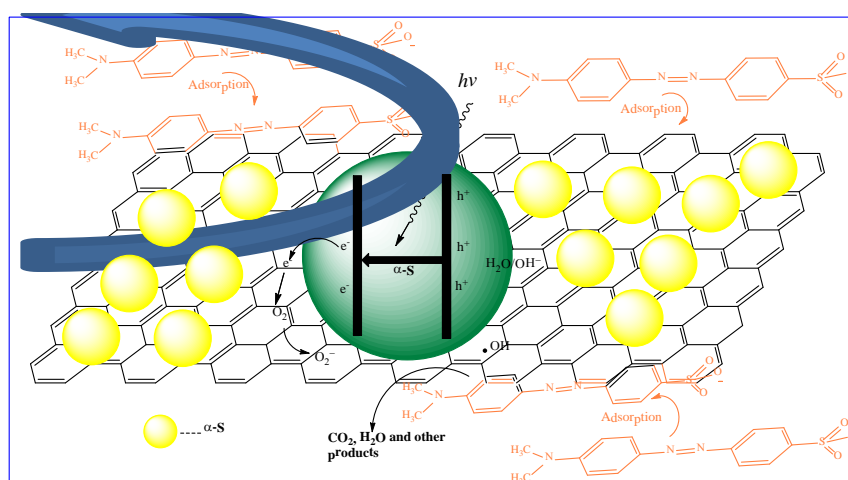
Figure 7 Schematics of the proposed reaction mechanism for the photocatalytic degradation of MO by the S/GR composite.

$$\alpha\text{-S} + h\nu \rightarrow \alpha\text{-S} (e^- + h^+) \qquad (1)$$
$$\alpha\text{-S} (e^-) + GR \rightarrow \alpha\text{-S} + GR (e^-) \qquad (2)$$
$$GR (e^-) + 1/2 O_2 \rightarrow GR + O_2^- \qquad (3)$$
$$\alpha\text{-S} (h^+) + MO \rightarrow CO_2 + H_2O + \text{other products} \qquad (4)$$
$$\alpha\text{-S} (h^+) + OH^- \rightarrow \alpha\text{-S} + \cdot OH \qquad (5)$$
$$\cdot OH + MO \rightarrow CO_2 + H_2O + \text{other products} \qquad (6)$$

4. Conclusions

The α-S/GR composite, a novel metal-free photocatalyst, was synthesized using a facial one-pot, two-step hydrothermal method. Compared with pure α-S, the new catalyst shows much enhanced photocatalytic activity for the degradation of MO under both UV and simulated solar light. The incorporation of GR greatly increases the hydrophilicity and adsorption capacity of α-S. Moreover, the graphene sheets can function as electron collectors to facilitate the electron–hole separation, resulting in enhanced $\cdot OH$ radical generation and MO degradation.

Acknowledgements

References

[1] Fujishima, A. Electrochemical photolysis of water at a semiconductor electrode. *Nature* **1972**, *238*, 37-38.

[2] Chen, X. B.; Shen, S. H.; Guo, L. J.; Mao, S. S. Semiconductor-based photocatalytic hydrogen generation. *Chem Rev* **2010**, *110*, 6503-6570.

[3] Wang, F.; Ng, W. K. H.; Yu, J. C.; Zhu, H. J.; Li, C. H.; Zhang, L.; Liu, Z. F.; Li, Q. Red phosphorus: An elemental photocatalyst for hydrogen formation from water. *Appl Catal B-Environ* **2012**, *111*, 409-414.

[4] Liu, G.; Niu, P.; Yin, L. C.; Cheng, H. M. Alpha-sulfur crystals as a visible-light-active photocatalyst. *J Am Chem Soc* **2012**, *134*, 9070-9073.

[5] Wang, X. C.; Maeda, K.; Thomas, A.; Takanabe, K.; Xin, G.; Carlsson, J. M.; Domen, K.; Antonietti, M. A metal-free polymeric photocatalyst for hydrogen production from water under visible light. *Nat Mater* **2009**, *8*, 76-80.

[6] Novoselov, K. S.; Geim, A. K.; Morozov, S. V.; Jiang, D.; Zhang, Y.; Dubonos, S. V.; Grigorieva, I. V.; Firsov, A. A. Electric field effect in atomically thin carbon films. *Science* **2004**, *306*, 666-669.

[7] Huang, X.; Qi, X. Y.; Boey, F.; Zhang, H. Graphene-based composites. *Chem Soc Rev* **2012**, *41*, 666-686.

[8] Xiang, Q. J.; Yu, J. G.; Jaroniec, M. Synergetic effect of MoS_2 and graphene as cocatalysts for enhanced photocatalytic H_2 production activity of TiO_2 nanoparticles. *J Am Chem Soc* **2012**, *134*, 6575-6578.

[9] Xiang, Q. J.; Yu, J. G.; Jaroniec, M. Graphene-based semiconductor photocatalysts. *Chem Soc Rev* **2012**, *41*, 782-796.

[10] An, X. Q.; Yu, J. C. Graphene-based photocatalytic composites. *Rsc Adv* **2011**, *1*, 1426-1434.

[11] Du, A. J.; Sanvito, S.; Li, Z.; Wang, D. W.; Jiao, Y.; Liao, T.; Sun, Q.; Ng, Y. H.; Zhu, Z. H.; Amal, R.; Smith, S. C. Hybrid graphene and graphitic carbon nitride nanocomposite: Gap opening, electron-hole puddle, interfacial charge transfer, and enhanced visible light response. *J Am Chem Soc* **2012**, *134*, 4393-4397.

[12] Hummers Jr, W. S.; Offeman, R. E. Preparation of graphitic oxide. *J Am Chem Soc* **1958**, *80*, 1339-1339.

[13] Paredes, J. I.; Villar-Rodil, S.; Martinez-Alonso, A.; Tascon, J. M. D. Graphene oxide dispersions in organic solvents. *Langmuir* **2008**, *24*, 10560-10564.

[14] Park, M. S.; Yu, J. S.; Kim, K. J.; Jeong, G.; Kim, J. H.; Jo, Y. N.; Hwang, U.; Kang, S.; Woo, T.; Kim, Y. J. One-step synthesis of a sulfur-impregnated graphene cathode for lithium-sulfur batteries. *Phys Chem Chem Phys* **2012**, *14*, 6796-6804.

[15] Fernandez-Merino, M. J.; Guardia, L.; Paredes, J. I.;

Villar-Rodil, S.; Solis-Fernandez, P.; Martinez-Alonso, A.; Tascon, J. M. D. Vitamin C is an ideal substitute for hydrazine in the reduction of graphene oxide suspensions. *J Phys Chem C* **2010**, *114*, 6426-6432.

[16] Zhang, Y. H.; Tang, Z. R.; Fu, X. Z.; Xu, Y. J. TiO_2-Graphene Nanocomposites for Gas-phase photocatalytic degradation of volatile aromatic pollutant: Is TiO_2-graphene truly different from other TiO_2-carbon composite materials? *Acs Nano* **2010**, *4*, 7303-7314.

[17] Nam, W.; Kim, J.; Han, G. Y. Photocatalytic oxidation of methyl orange in a three-phase fluidized bed reactor. *Chemosphere* **2002**, *47*, 1019-1024.

[18] Zhang, H.; Lv, X. J.; Li, Y. M.; Wang, Y.; Li, J. H. P25-graphene composite as a high performance photocatalyst. *Acs Nano* **2010**, *4*, 380-386.

[19] Liu, J. C.; Bai, H. W.; Wang, Y. J.; Liu, Z. Y.; Zhang, X. W.; Sun, D. D. Self-assembling TiO_2 nanorods on large graphene oxide sheets at a two-phase interface and their anti-recombination in photocatalytic applications. *Adv Funct Mater* **2010**, *20*, 4175-4181.